Adsorption Science & Technology

Research Article

Adsorption Science & Technology
2020, Vol. 38(9–10) 464–482

DOI: 10.1177/0263617420957829
journals.sagepub.com/home/adt
SAGE

Removal of brilliant green (BG) by activated carbon derived from medlar nucleus (ACMN) – Kinetic, isotherms and thermodynamic aspects of adsorption

Moussa Abbas
Laboratory of Soft Technologies and Biodiversity, Faculty of Sciences, University M'hamed Bougara of Boumerdes, Boumerdes, Algeria

Abstract

Experimental investigations were undertaken to adsorb Brilliant Green (BG) a toxic dye from aqueous medium using activated carbon derived from the medlar nucleus (ACMN). The adsorption was used to remove BG using ACMN as bio-adsorbent to replace activated carbon still expensive. The prepared adsorbent was characterized by the BET surface area measurement, FTIR spectroscopy and X-ray diffraction. Various parameters such as the initial dye concentration (110–200 mg/L), adsorbent dose (1–6 mg/L), initial pH (2–9) and temperature (298–318 K) were studied to observe their effects on the BG adsorption. Batch studies were conducted in order to determine the optimal parameters required to reach the adsorption equilibrium. The maximum adsorption capacity of ACMN for the BG adsorption at 298 K was found to be 833.15 mg/g. The adsorption kinetic data were analyzed by using several kinetic models namely the pseudo-first-order, pseudo-second-order, Elovich equation, intraparticules diffusion model. It was established that the adsorption obeys the pseudo-second-order kinetic model. The evaluation of thermodynamics parameters such as the free energy ΔG° (-10.584 to -6.413 kJ/mol), enthalpy ΔH° (36.439 kJ/mol) and the change of entropy (0.1438 kJ/mol K) indicated a spontaneous and endothermic nature of the reaction with a chemisorption process. The present adsorbent may be considered as an alternative for the better performance of the BG removal from aqueous medium.

Corresponding author:
Moussa Abbas, Laboratory of Soft Technologies and Biodiversity, Faculty of Sciences, University M'hamed Bougara of Boumerdes, Boumerdes 35000, Algeria.
Email: moussaiap@gmail.com

Keywords
Kinetic, isotherm, adsorption, thermodynamic, Nefles nucleus, brilliant green, modeling

Submission date: 23 March 2020; Acceptance date: 20 August 2020

Introduction

Dyes are colored organic compounds which are discharged in sewage water from many industries, such as paper, fabrics, leather, cosmetics, and printing. The long-time adverse environmental effects caused by discharging these dyes change the water color and sunlight permeation; they are unpleasant for both drinking and domestic uses. Dye molecules usually consist of complex aromatic frameworks and exhibit bright colors. Such aromaticity exhibits a long-term stability, thus preventing biodegradation (Abbas and Trari, 2020a). Extensive and versatile usage of dye generates serious pollution problems in environmental water. Dyes mainly enter food products via industrial emissions causing serious health hazards (Abbas et al., 2020; Ahn et al., 1999). The great visibility of dyes, even at trace concentrations is generally linked to less-dissolved oxygen in aquatic habitats, decreasing the penetration of sunlight along with photosynthetic activities. In this way, ecological damage can spread downstream to agricultural or aquaculture regions, affecting aquatic flora and fauna. It is therefore compulsory for certain places to exercise an appropriate treatment before the disposal of this wastewater (Abbas and Trari , 2020b). Brilliant green BG products include a group of dye compounds which have many uses namely biological staining, dermatological agent, veterinary medicine, and inhibitor of mold/intestinal parasites/fungus propagation. The global demand for coatings and paints is predicted to rise 3.7% per year with 54.7 million metric tons in 2020. The growing consumer demand for the dye compounds in various end-use segments (such as plastics, textiles, food, and paints & coating) is projected to act as a major growth factor for the global market over the following few years. Accumulation of dyes in the environment, as almost indestructible toxicants, is therefore a great concern. BG, a widely used dye, travels to incorporate the aquatic systems owing to its high solubility (100 g/L). It pollutes also the atmosphere because of its high volatility. So, the development of green recycling processes is justified. Brilliant green BG appears as a golden crystal and organic dye that belongs to the triphenyl methane family. It has many uses, such as dermatological agent, biological stain, veterinary medicine, and intestinal parasites (Nandi et al., 2009). Brilliant green is toxic when injected into humans and animals. Common harmful effects of BG on humans are irritation to the gastrointestinal tract with long-term exposure resulting in organ damage (Mittal et al., 2008). As a result of its decomposition, sulphur oxides, nitrogen oxides, and carbon dioxide are produced which further pollute the environment (Kismir and Aroguz, 2011).The recovery of agricultural residues without generating pollutants is a great challenge and is recommended for sustainable industrial development in order to preserve the natural environment. All inexpensive materials such as biomass wastes: apple peel (Suárez-García et al., 2001), date pits (Ahmed and Dhedan, 2012), olive pits (Berrios, et al., 2012), peach pits (Attia et al., 2008), pomegranate peels (Abbas et al., 2020), coffee beans (Baquero et al., 2003) and coffee grounds (Kyzas et al., 2012), tea scraps (Yagmur et al., 2008), bagasse (Valix et al., 2004), coconut shell (Laine et al., 1989) and kernels 'apricot (Harrache et al., 2019) with a high

carbon content can be used as precursors for the production of activated carbon. These cheaper and renewable precursors were compared to commercial activated carbon (Abbas and Trari , 2020c). The preparation of an activated carbon from the medlar nucleis and the optimization of the parameters influencing the adsorption of the dye BG are the main objective of this study. A comparative study showed that this adsorbent can constitute a new support in the treatment of waters.

Materials and methods

Materials

Nuleis were obtained from the Boumerdes region (50 km east of Algiers). After properly cleaning the nuleis with double distilled water, they remained at room temperature for 2 days for drying. Then, they were ground to have particles smaller than 50 mesh and placed in brown bottles for future use. The brilliant green BG(chemical formula $C_{27}H_{34}N_2O_4S$;482.63 g/mol; purity 99.998%) was provided by Merck Company. The IUPAC Name is [4-[[4-(diethylamino) phenyl]-phenylmethylidene]cyclohexa-2,5-dien-1-ylidene]-diethylazanium;hydrogen sulfate. Dye stock solution (1000 mg/L) was prepared by dissolving the BG powder in distilled water. The solutions at required concentration were adjusted by dilution for adsorption experiments. The chemical properties of the dye are listed in the Table 1.

Preparing activated carbon ACMN

The purification of the Medlar Nuclei was washed several times with distilled water until the odor disappeared and clear rinsed water was obtained. The cores were dried for 24 h at 110°C in an air oven. Then, they were crushed and sieved, washed several times with distilled water to remove impurities and dried at 110°C (24 h). Finally, the powder has undergone activation with H_3PO_4. The latter has been widely used for the activation of carbon (Baccar et al., 2012; Sun et al., 2012; Liou, 2010). For this, 10 g of crude sample medlar nuclei was mixed with 20 g of the H_3PO_4 solution (40% wt.) and kept under magnetic stirring for 2 h. The mixture was placed in the oven for 24 h at 110°C. The product was placed in a calcinations oven, with a heating rate of 10°C/min and kept at temperature 450°C for (1 h).

Table 1. Chemical proprieties of brilliant green (BG).

Brute Formula	$C_{27}H_{25}N_2NaO_7S_2$
Molecular weight (g/mol)	576.616
pKa	2.62–4.93
I.C	42,040
Composition (%)	C: 56.24, N: 4.86, O: 19.42 H: 4.370, Na: 3.99, S: 11.12
Wavenumber λ_{max} (nm)	624
Name	Acid Green Brilliant Green
Solubility in water (g/L)	25 at T = 20°C
Solubility in alcohol	Very soluble

The product obtained was washed with distilled water several times until the pH of the supernatant becomes 6.5. The product is then dried at 110° C for 24 h. The sample obtained is noted: Activated carbon prepared from Medlar Nuclei (ACMN).

Characterization of prepared activated carbon ACMN

Adsorption–desorption experiments were performed at liquid N_2 temperature (-196.15°C) by means of Micromeritics Tri Star II 3020. To remove volatile contaminations, degassing processes were completed for EACs at 90°C for 0.5 h and immediately after, at 300°C for 2 h under vacuum. By using the BET method, the specific surface areas were determined, and total pore volumes were calculated through N_2 adsorption at $P/P_o = 0.984$.

The Fourier Transform Infrared spectroscopy (FTIR) was used to identify the characteristic functional groups of the natural Medlar nuclei (NMN), Basic Medlar nuclei (BMN) and acid Medlar nuclei ACMN. 5 mg of adsorbent was mixed with dry KBr of spectroscopy quality and pressed under 4500 psi to form thin disc. Then, the FTIR spectrum was plotted with a Perkin Elmer 2000 infrared spectrometer in the range (4000–400 cm^{-1}) for 16 times to increase the signal to noise ratio.

The X-ray diffraction (XRD) of NMN, BMN and ACMN was done with a Philips X-ray diffractometer (PW 1890 model) 40 kV, 40 mA, $\lambda = 1.54$ Å. The patterns were obtained with CONIT T-2T scan mode at 0.17 deg/step of step width and 8°/min of scan speed.

The point of zero charge (pHpzc) is important in adsorption, especially when electrostatic forces are involved in the mechanisms. pHpzc was measured as follows: 50 mL of KNO_3 solution (0.01 M) was placed in Erlenmeye flasks including 0.1 g of ACMN. The initial pH was adjusted between 2 and 11 by addition of NaOH or HCl (0.1 N). After a contact time of 48 h under magnetic agitation, the ultimate pH was determined and plotted versus the initial pH (Abbas et al., 2018).

Adsorption experiments

The adsorption experiments were performed in batch mode. In batch adsorption studies, the dye solutions at the desired concentrations were adjusted from the BG stock solutions by dilution and placed in Erlenmeyer flasks to which the adsorbent was added. They were placed in a shaker with thermostat controlled (Wise Bath) and shaken at 250 rpm until the adsorption equilibrium was reached at desired temperature. Samples were then centrifuged for 20 min at 4000 rpm to set apart their solid phases from liquid phases; the remaining dye concentrations were titrated after centrifugation by using a UV–visible spectrophotometry (Mecasys Optizen POP Series) at 624 nm (λ_{max}) using the above method.

The effect of the initial dye concentration (C_0: 110–200 mg/L), adsorbent dose ACMN (0.05–0.3 g/50 mL, (1–6 mg/L), initial pH (2–9) and temperature (298–318 K) on the BG adsorption was studied. The amount of BG (mg/g) adsorbed by ACMN (q_t) was calculated from the relation:

$$q_t = \frac{(C_0 - C_t) \cdot V}{m} \tag{1}$$

where C_0 is the initial BG concentration and C_t the concentrations (mg/L) at time t, V the volume of solution (L) and m the mass of ACMN (g).

Results and discussion

Adsorbent characterization

BET surface area and pore size. The specific surface area was determined by the BET equation. The external surface area, micropore area and micropore volume were calculated by the *t*-plot method. The total pore volume was evaluated from the liquid volume of N_2 at high relative pressure near unity 0.99. The mesopore volume was computed by subtracting the micro-pore volume from the total volume. The pore size distribution (PSD) was determined from the density functional theory (DFT) model. All characteristics for the adsorbent (ACMN) are reported in Table 2.

X-ray diffraction analysis. Figure 1(a) shows the amorphous structure and low crystallinity of all samples in the range (10–43°). For the raw material, the pattern has a peak at 22°,

Table 2. Physicochemical characteristics of ACMN.

Humidity (%)	Ash rate (%)	pHpzc
1.8	2.3	2.20
S_{BET} (m^2/g)	1409	
S_{ExT} (m^2/g)	204	
S_{mic} (m^2/g)	1205	
VPT (m^3/g)	1.174	
V_{mic} (cm^3/g)	0.786	
V_{mes} (cm^3/g)	0.338	
V_{mic} (%)	66.95	
V_{mes} (%)	33.05	

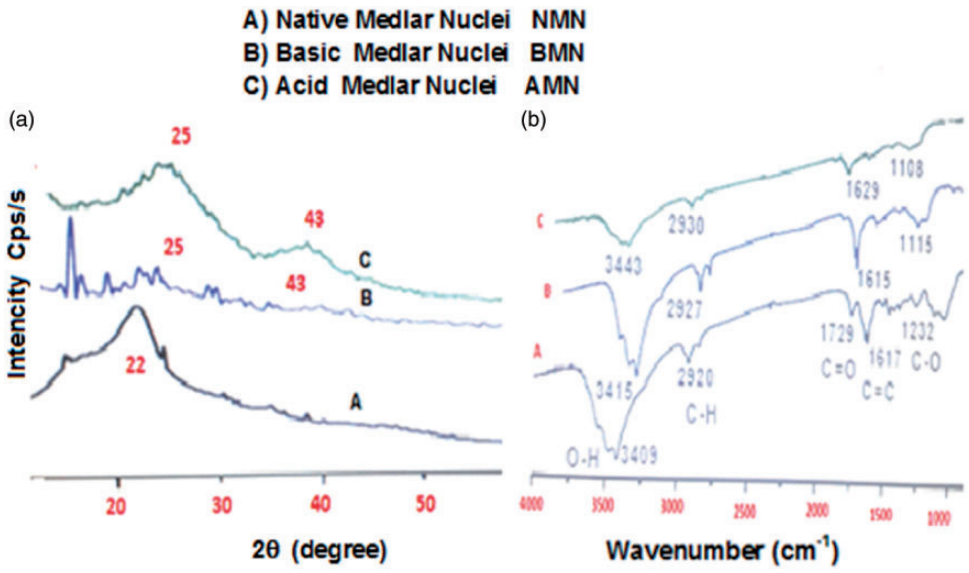

Figure 1. (a) XRD spectrum of different adsorbent. (b) FTIR spectrum of different adsorbent.

attributed to the presence of native cellulose. The patterns of different activated carbons, AMN and raw NMN (native) show almost the same shape with the same diffraction peaks at 25 and 43° which assigned respectively to the presence of carbon/graphite and dehydrated hemicelluloses (Djilani et al., 2012). On the other hand, we note that after activation of the raw materials, the main peak moves from 22 to 25° with the appearance of a peak at 43°, indicating that the activation process was successfully completed.

FTIR spectrum analysis. Figure 1(b) shows that the bands (C – H) at 2930 and 2850 cm^{-1} are much weaker for BMN (Basic Medlar Nuclei)The small peak at 1700 cm^{-1} is attributed to the stretching vibrations of the C = O groups (cetones, aldehydes, lactones or carboxylic groups). The spectra also show a band (1650–1600 cm^{-1}) due to the vibrations of elongation of C = C bond in the olefin structure, the peaks between 1000 and 1350 cm^{-1} are assigned to the vibrations of CO bonds (Liou, 2010). We observe a small decrease in the intensity of the peaks 1740 cm^{-1} of the synthesized materials and the disappearance of another at 2920 cm^{-1} for BMN due to carbonization.

Influence of analytical parameters

Influence of the contact time and initial concentration on the adsorption capacity. The adsorption capacity of BG increases over time to reach a maximum after 60 min of contact time (Figure 2) and thereafter tends toward a constant value indicating that no more BG ions are adsorbed from the solution. The equilibrium time averages 50 min but for practical reasons the adsorption experiments are run up to 60 min. From these results, one can deduce that the adsorption of BG onto ACMN is done in three stages; a rapid adsorption during the first minutes of interaction; this can be interpreted by the fact that at the start of adsorption, the number of active sites available on the adsorbent surface is much greater than that of the remaining sites (Dincer et al., 2006; Abbas, 2020). For the high contact

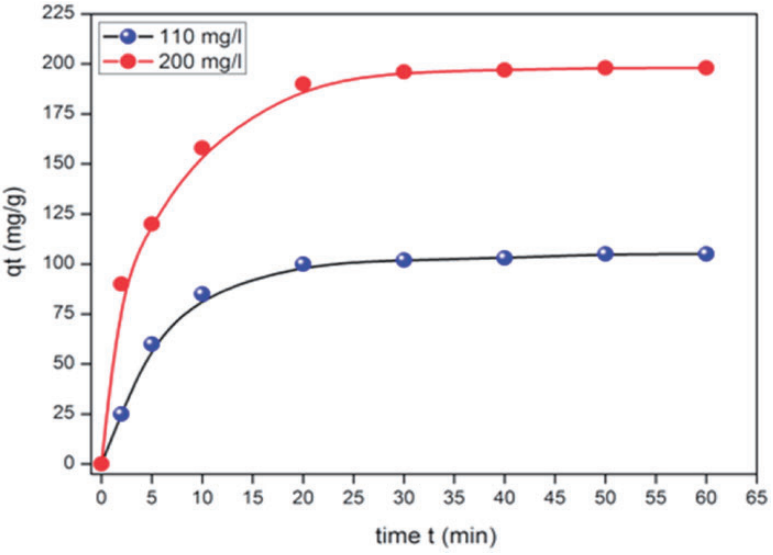

Figure 2. Evolution of the adsorption of BG dye onto ACMN as a function of time and concentration.

times, the molecules need more time to diffuse inside the pore of the adsorbent (Abbas et al., 2019), For the rest, the no adsorption is interpreted by the saturation of the surface of the adsorbent (all adsorption sites are occupied).

Influence of pH on adsorption capacity. The pH of the solution plays an important role in the adsorption process, particularly on the uptake capacity (Tavlieva et al., 2013), it influences the quantity adsorbed according to the following parameters:

The charge of the adsorbent surface, the degree of ionization of the adsorbate and the degree of dissociation of the functional groups from the active sites of the adsorbent (Nandi et al., 2009). To study the influence of pH on the BG adsorption by unaccompanied minors, we used 50 mL of the concentration (100 mg/L) for different pH, a temperature 25°C and a contact time of 50 min, the quantity of ACMN of 50 mg.It is observed that the percentage of BG removal increasing consistently with increasing pH (Figure 3(a)). The effect of pH on the BG adsorption by ACMN can be explained on the basis of $pH_{(pzc)}$(=2.2) . An increase in the adsorbed amount of BG when the pH increases. This change in the adsorbed quantity in the studied pH range can be explained by the fact that at pH higher than pHpzc, the surface of activated carbon is negatively charged and the BG molecules are positively charged (Colak et al., 2009).

The adsorption is attributed to attractive electrostatic interactions adsorbent/pollutant. These interactions increase with raising pH because the surface of coal becomes more and more negative when the solution becomes more basic.

The effect of the adsorbent dosage ACMN. The first stage of batch experiments and the effect of adsorbent dose on the BG adsorption onto ACMN are examined. Significant variations in the uptake capacity and removal efficiency are observed at different adsorbent dose (1–6 g/L), indicating that the best adsorption is obtained for a dose of 1 g/L (Figure 3(b)). This result was subsequently used in all isotherms adsorption experiments.

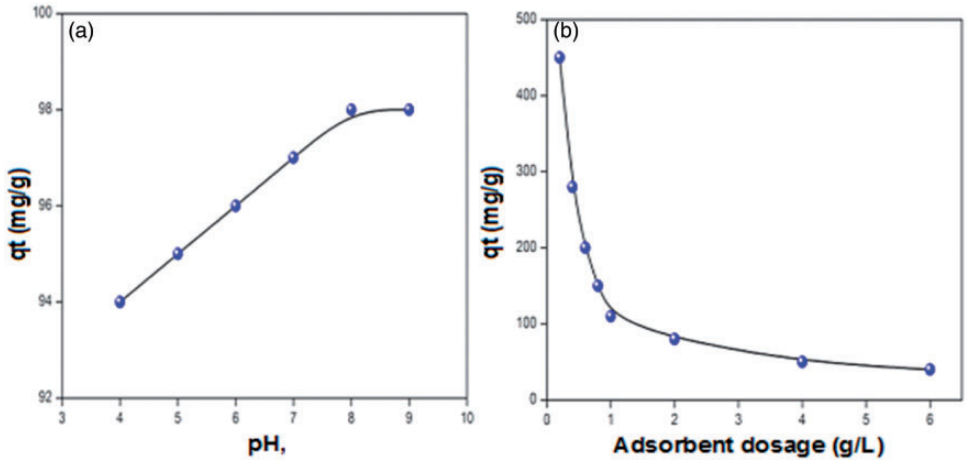

Figure 3. (a) Evolution of the adsorption of BG dye onto BG as a function of pH. (b) Evolution of the adsorption of BG dye onto ACMN as a function of adsorbent dosage.

Adsorption kinetic study. The kinetic study is important since it describes the uptake rate of adsorbate and controls the residual time of the whole process. Several models were proposed to study the mechanisms controlling the adsorption. In this study, the experimental data of BG adsorption are examined using a pseudo-first and pseudo-second order kinetic model; the pseudo-first order equation (Lagergren, 1998) is given by the equation:

$$\log(q_e - q_t) = \log q_e - \frac{K_1}{2.303} \cdot t \tag{2}$$

The pseudo second order model (Ho and McKay, 1998) is expressed by the equation:

$$\frac{t}{q_t} = \frac{1}{K_2 \cdot q_e^2} + \frac{1}{q_e} \cdot t \tag{3}$$

where q_t (mg/g) is the amount of BG adsorbed on ACMN at the time t (min). K_1 (min^{-1}) and K_2 (g/mg·min) are the pseudo-first order and pseudo-second order kinetics constants respectively. The slope and intercept of the plots $\ln(q_e - q_t)$ *vs.* t and t/q_e *vs.* t were used to determine the first-order rate constants K_1 and q_e and second-order rate constants K_2 and q_e respectively.

The rate constants predict the uptakes and the corresponding correlation coefficients for ACMN summarized in Table 3. For the pseudo-first-order kinetic (Figure 4(a)), the experimental data deviate from linearity, as evidenced from the low values of q_e and C_o and therefore the model is inapplicable for the present system. By contrast, the correlation coefficient and $q_{e,cal}$ determined from the pseudo-second order kinetic model agree with the experimental data (Figure 4(b)) and its applicability suggests that the adsorption BG onto ACMN is based on chemical reaction i.e. chemisorption, involving an exchange of electrons between adsorbent and adsorbate. The dye BG is attached to the adsorbent surface by chemical bond and tends to find sites that maximize their coordination number with the surface.

The Elovich kinetic equation is related to the chemisorptions process (Figure 5(a)) and is often validated for systems where the surface of the adsorbent is heterogeneous (Juang and Chen, 1997); the linear form is given by:

$$q_t = \left(\frac{1}{\beta}\right) \mathrm{Ln}\ \alpha.\beta + \left(\frac{1}{\beta}\right) \mathrm{Lnt} \tag{4}$$

where α (mg/g min) is the initial adsorption rate, and β (mg/g) the relationship between the degree of surface coverage and the activation energy involved in the chemisorption.

Intra-particle diffusion equation. The study of adsorption kinetics is important because the rate of adsorption, which is one of the criteria for determining the efficiency of an adsorbent, and the mechanism of adsorption can both be determined from the kinetic studies. As a standard parameter for studying the behavior of BG adsorption onto ACMN surface is obtained using the Morris-Weber equation (Weber and Morris, 1963):

$$q_t = K_{in}\sqrt{t} + C \tag{5}$$

Table 3. Pseudo first-order, pseudo second-order, Elovich and intraparticules models constants and determination coefficients for BG adsorption onto ACMN.

	Second	Order				Pseudo 1	Order		
C_o (mg/L)	q_{ex} (mg/g)	q_{cal} (mg/g)	R^2	RSS	K_2 (g/mg.mn)	q_{cal} (mg/g)	R^2	RSS (%)	K_1 (mn^{-1})
110	105.00	114.81	0.9956	0.0009	0.00188	75.333	0.9272	0.1798	0.1029
200	198.00	209.64	0.999	0.0001	0.00168	152.155	0.9833	0.0668	0.1345
Elovich					Diffusion				
C_o (mg/L)	R^2	β (g/mg)	α (mg/g.mn)	SSE	K_{in} (mg/g.$mn^{1/2}$)	R^2	C ($mn^{1/2}$)		RSS
110	0.8961	0.0437	56.284	522.026	23.948	0.9502	–0.9502		256.55
					0.6296	0.9696	131.92		0.0741
200	0.9351	0.0295	285.71	689.730	42.110	0.947	16.559		843.16
					0.6296	0.866	–57.789		0.2552

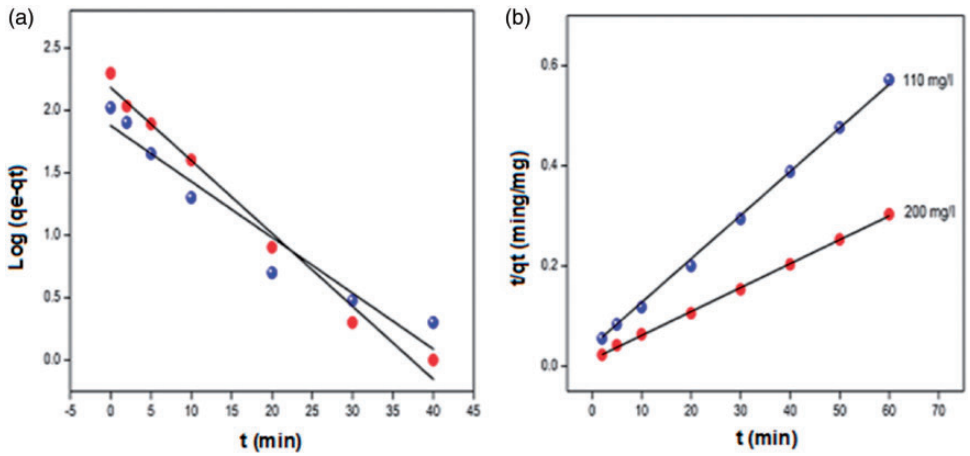

Figure 4. (a) First-order Kinetic model fit for the adsorption of BG dye onto ACMN. (b) Pseudo-second-order model fit for the adsorption of BG dye onto ACMN.

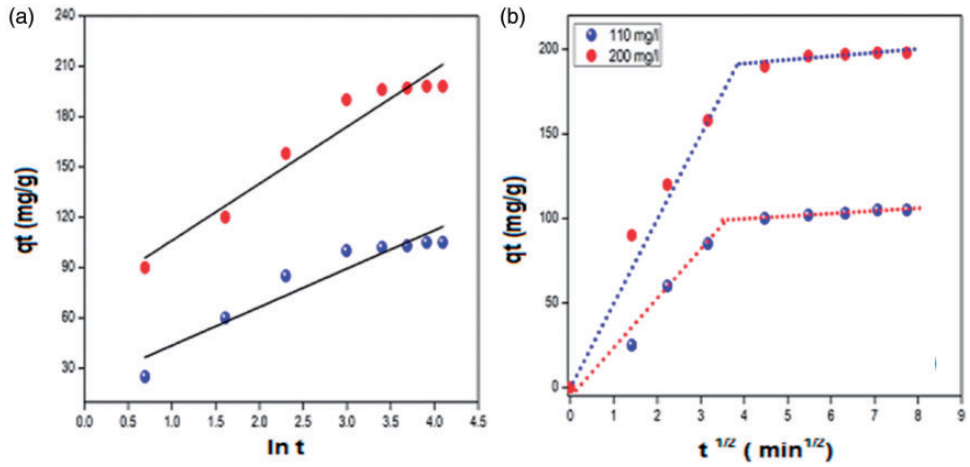

Figure 5. (a) Elovich model for the adsorption of BG dye onto ACMN. (b) Intra-particle diffusion model for the adsorption of BG dye onto ACMN.

where K_{id} is the intra-particle diffusion rate constant (mg/g $min^{1/2}$), q_t the amount of BG dye sorption at time t and C (mg/g) the intercept. The plot of q_t versus $t^{1/2}$ enables to determine both K_{id} and C. Figure 5(b) presents a multi-linearity correlation, which indicates that two steps occur during the BG adorption. The Morris-Weber model reveals an initial linear portion which may be due to the boundary layer effect while the second portion which may be due to the intraparticle diffusion effect. The mechanism of adsorption is complex but the intraparticle diffusion is important in the early stages. The first linear portions could be due to intra-particle diffusion effects. The slopes of the linear parts are defined as rate parameters, characteristic of the adsorption rate in the region where the intraparticle diffusion occurs.

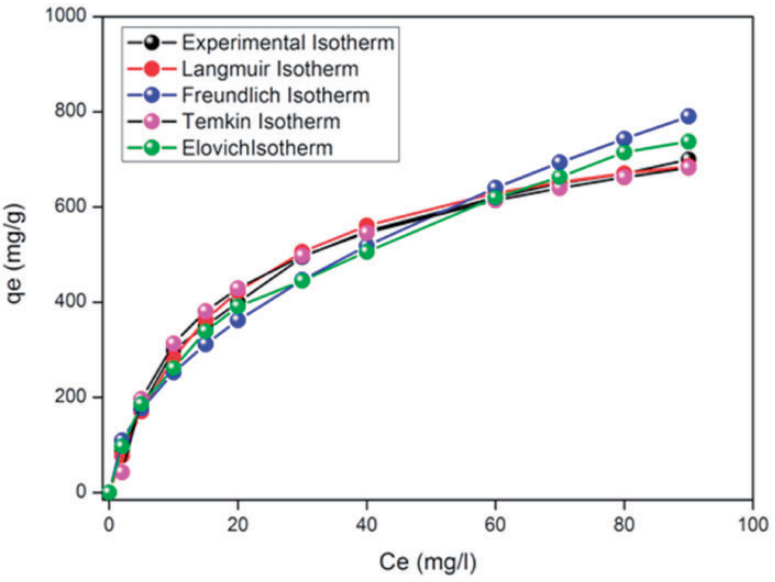

Figure 6. Non Lineair Isotherms models in the optimum conditions.

Initially and within a short-time period, it is postulated that BG is transported to the external adsorbent surface through the film diffusion with a high rate.

After saturation of the surface, the BG ions enter inside the adsorbent by intra-particle diffusion through the pores and internal surface diffusion until equilibrium is reached which is represented by the second straight lines. The constants of the different models deduced after modeling are grouped in Table 3.

Adsorption equilibrium isotherms. To assess the performance of ACMN, different isotherms exist, among which the Langmuir (Langmuir, 1918), Freundlich (Freundlich, 1906), Temkin (Temkin and Pyzhev, 1940), and Elovich (Ghaedj et al., 2013) isotherms were used that have been presented in Figure 6. Besides, the isotherm models were applied at optimal conditions of the parameters.

The Langmuir model is the best known and most widely applied, it is represented by the non linear and linear forms:

$$q_e = \frac{q_{\max} \,.\, K_L \,.\, C_e}{1 + \; K_L.C_e}$$

$$\frac{1}{q_e} = \frac{1}{q_{\max}} - \frac{1}{q_{\max} \,.\, K_L.\, C_e} \tag{6}$$

where C_e is the equilibrium concentration (mg/L), $q_{\max}$ the monolayer adsorption capacity (mg/g) and K_L the constant related to the free adsorption energy (L/mg) Figure 7(a).

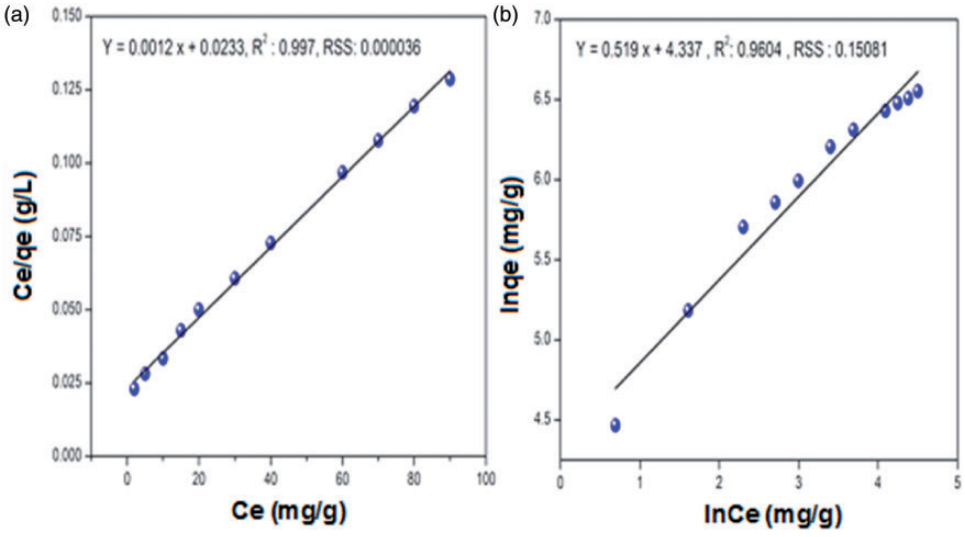

Figure 7. (a) Fitted Langmuir Isotherm model in the optimum conditions. (b) Fitted Freundlich Isotherm model in the optimum conditions.

The applicability to the adsorption is compared by evaluating the statistic RSS and R^2 values at 25°C. The smaller RSS values obtained for the models indicate a better fitting. The essential features of the Langmuir model

$$R_L = \frac{1}{1 + K_L \cdot C_0} \tag{7}$$

where C_o is the initial concentration of the adsorbate in solution. R_L indicates the type of isotherm: irreversible ($R_L = 0$), favourable ($0 < R_L < 1$), linear ($R_L = 1$) or unfavourable ($R_L > 1$). In this study, the R_L values are smaller than 1, thus confirming that the adsorption is favoured in both cases as well as the applicability of the Langmuir isotherm.

The Freundlich isotherm is valid for non ideal adsorption on heterogeneous surfaces as well as multilayer sorption.

$$qe = K_F . C_e^{1/n}$$

$$\ln q_e = \ln K_F + \frac{1}{n} \cdot \ln C_e \tag{8}$$

The constant K_F characterizes the adsorption capacity of the adsorbent (L/g) and n an empirical constant related to the magnitude of the adsorption driving force. Therefore, the plot $\ln q_e$ versus $\ln C_e$ (Figure 7(b)) enables the determination of both the constant K_F and n.

The Temkin isotherm describes the behavior of adsorption systems on heterogeneous surfaces, it is applied in the following form:

$$q_e = (RT/b).\ln(AC_e)$$

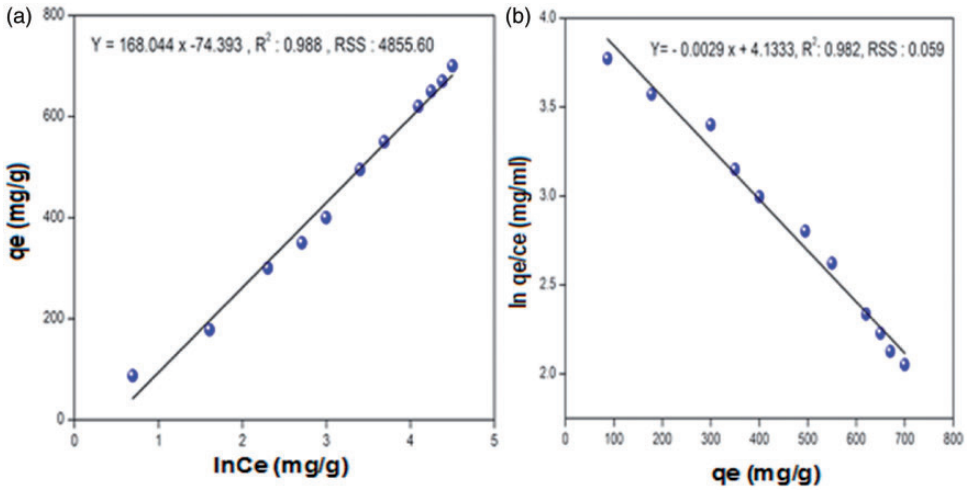

Figure 8. (a) Fitted Temkin Isotherm model in the optimum conditions. (b) Fitted Elovich Isotherm in the optimum conditions.

$$q_e = B_T \ln C_e + B_T \ln A_T \tag{9}$$

The adsorption data are analyzed according to equation (9). Therefore, the plot q_e versus lnCe enables to determine the constants A_T and B_T (Figure 8(a)).

The Elovich isotherm is based on the principle of the kinetic, assuming that the number of adsorption sites augments exponentially with the adsorption; this implies a multi layer adsorption described by:

$$\frac{q_e}{q_{\max}} = K_E.\mathrm{Ce}\,.\exp\left(-\frac{q_e}{q_{\max}}\right)$$

$$\ln\frac{q_e}{C_e} = \ln(q_m\,.K_E) - \frac{q_e}{q_{\max}} \tag{10}$$

where K_E (L/mg) is the Elovich constant at equilibrium, $q_{\max}$ (mg/g) the maximum adsorption capacity, q_e (mg/g) the adsorption capacity at equilibrium and C_e (g/L) the concentration of the adsorbate at equilibrium. Both K_E and $q_{\max}$ are calculated from the plot of ln (q_e/C_e) versus q_e (Figure 8(b)). The constants of the different models are gathered in Table 4.

Thermodynamic study

The thermodynamic properties were investigated to determine whether the adsorption process occurred spontaneously. The thermodynamic parameters, namely, standard enthalpy (ΔH°, kJ/mol), standard entropy (ΔS°, J/mol K), and standard free energy (ΔG°, kJ/mol), were calculated using the following equations (Abbas et al., 2020):

$$\Delta G^\circ = \Delta H^\circ - T\Delta S^\circ \tag{11}$$

Table 4. Parameters of the adsorption isotherms for BGdye onto ACMN.

25°C	Langmuir	Freundlich	Temkin	Elovich
K_L	0.0515 L/mg	1/n: 0.519	B_T: 168.044	K_E: 0.1809 L/mg
q_{max}	833.33 mg/g	n: 1.926	A_T: 0.644 L/mg	q_{max}: 344.83 mg/g
		K_F: 76.477 mg/g	ΔQ: 12.295 KJ/mol	
R^2	0.997	0.9604	0.988	0.982
RSE	0.00004	0.1508	4855.6	0.059

RSS: Residual Sun of Squart, R^2: Determination coefficient, ΔQ: Temkin Energy.

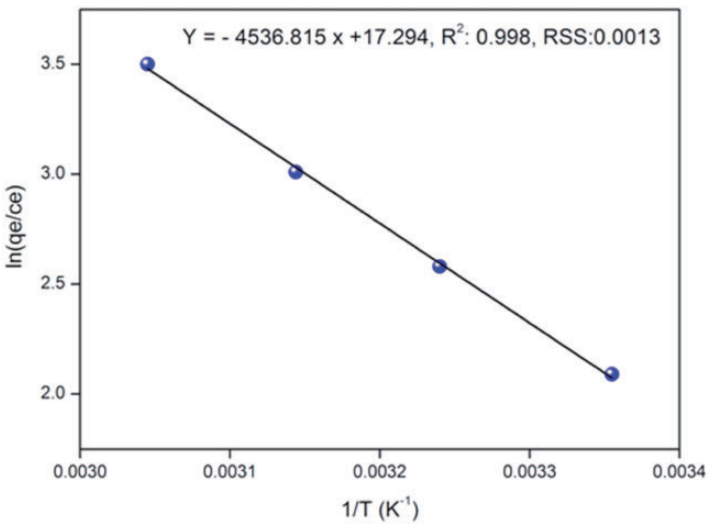

Figure 9. Regression of Van't Hoff for thermodynamic parameters of BG adsorption on ACMN.

$$\Delta G^\circ = -RT \ln K_d \tag{12}$$

$$K_d = \frac{qe}{Ce} \tag{13}$$

$$\ln K_d = -\frac{\Delta H^\circ}{RT} + \frac{\Delta S^\circ}{R} \tag{14}$$

where R is the gas constant (8.314 J/mol K), T (K) the absolute temperature, K_d the distribution coefficient, q_e (mg/g) the quantity of BG adsorbed at equilibrium and C_e (mg/L) the quantity of BG remaining in solution at equilibrium. The equilibrium constant K_d was determined by plotting q_e/C_e versus C_e and extrapolating to zero q_e,. ΔH° and ΔS° obtained from the slope and intercept of the plots lnK versus 1/T (Figure 9) and ΔG° values at various temperatures are summarized in Table 5.

Table 5. Thermodynamic functions $\Delta G°$, $\Delta S°$ and $\Delta H°$ of BG adsorbed on the ACMN.

T (K)	1/T (K^{-1})	ln(qe/Ce)	K_d	$\Delta H°$ (kJ/mol)	$\Delta S°$ (kJ/K.mol)	$\Delta G°$ (k J/mol)
298	0.003413	2.0873	8.0631			–6.4130
308	0.003247	2.5766	13.152			–7.8514
318	0.003145	3.0066	20.218	36.439	0.1438	–9.2890
328	0.003049	3.5051	33.281			–10.584

Table 6. Comparison of maximum adsorption capacities for BG dye with literature data.

Adsorbents	q_m (mg/g)	Reference
Saklikent Mud	1.18	Kismir and Aroguz (2011)
Modified Chitosan	10.91	Karaer and Uzun (2013)
Hydrogel Loaded with Kalonite	26.31	Shirsath et al. (2013)
Kaolin	65.42	Nandi et al. (2009)
Red Clay	125.2	Saif Ur Rehman et al. (2013)
Yemen Natural Clay	476.4	Nassar et al. (2012)
Nano Hydroxyapatite/Chitosan Composite	49.11	Ragab et al. (2019)
Modified *Bambusa Tulda*	41.67	Laskar and Kumar (2019)
Novel Acorn based Adsorbent	2.11	Ghaedi et al. (2011)
AC Medlar Nuclei (ACMN)	**833.15**	This study

Performance of the prepared AMN

In order to enhance the value of our adsorbent, we carried out a comparative study of the maximum adsorption capacity obtained for the same pollutant to other adsorbents and activated carbon reported in the literature. Table 6 grouped together the different values of q_{max} for the different adsorbents. We can see that the BG adsorption observed in the present study is well positioned with respect to other researches with a maximum adsorption capacity q_{max} of 833.15 at 298 K, relatively interesting compared to other adsorbents. The differences of the BG uptakes are due to the morphological properties of each adsorbent like the structure, the functional groups and the surface area. ACMN could be an attractive adsorbent for basic dyes owing to its isoelectric point pH_{pzc}. The desorption is an unavoidable process and is an intermediate stage toward the adsorbent regeneration. The latter is an essential point to estimate the reutilization of any adsorbent for industrial applications, owing to the ecological concerns and the needs for sustainable development.and we wish to carry out column adsorption tests under the conditions applicable to the treatment of industrial effluents and to test the homogeneous photodegradation of BG on the SnO_2, TiO_2 semiconductors is the future objective of this work.

Conclusion

In this work, an experimental study on the utilization of Activated Carbon derived from Medlar Nuclei (ACMN) for the removal of Brilliant green from aqueous solution was

investigated. The following conclusions were made based on the experimental results of the present study:

The Activated Carbon was characterized by the Fourier transform infrared spectroscopy (FTIR), X-ray diffraction analysis (XRD) and BET method.

The potential of this adsorbent was studied for the decolonization of BG; the influence of the initial pH, dye BG concentration, contact time, adsorbent dose and temperature on adsorption of BG was investigated.

The adsorption capacity of BG increased with increasing the initial dye concentration, while the optimized pH was found to be 4.The kinetics of BG removal indicated an optimum contact time of 50 min via a two stage of adsorption kinetic profile (initial fast and subsequent slow equilibrium).

The BG adsorption onto ACMN follows a pseudo-second order kinetic model with a determination coefficient (R^2) very close to unity (=0.999). That relies on the assumption that the chemisorption may be the rate-limiting step and where the BG ions are attached to the adsorbent surface by forming chemical bonds and tend to find sites that maximize their coordination number with the surface.

The equilibrium adsorption data for BG on ACMN were analyzed by various models. The results indicate that the Langmuir isotherm provides the best correlation ($q_{max} = 833.15$ mg/g at 299 K).

The negative free enthalpy ΔG° and positive enthalpy ΔH° indicate that the adsorption of BG onto ACMN is spontaneous and endothermic over the studied temperatures range. BG is strongly bonded to the adsorbent surface while the positive entropy ΔS° states clearly that the randomness increases at the solid-solution interface during the BG adsorption and some structural exchange between active sites and BG ions.

The comparison of the adsorption capacity of our adsorbent with others showed its attractive properties from both industrial and economic interests. This study has given encouraging results.

Acknowledgements

The authors gratefully acknowledge support from University M'hamedBougara of Boumerdes, Laboratory of Soft Technologies and Biodiversity, Faculty of Sciences.

Declaration of Conflicting Interests

The author(s) declared no potential conflicts of interest with respect to the research, authorship, and/or publication of this article.

Funding

The author(s) received no financial support for the research, authorship, and/or publication of this article.

ORCID iD

Moussa Abbas https://orcid.org/0000-0002-0420-2414

References

Abbas M (2020) Experimental investigation of activated carbon prepared from apricot stones material (ASM) adsorbent for removal of malachite green (MG) from aqueous solution. *Adsorption Science & Technology* 38(1–2): 24–45.

Abbas M, Aksil T and Trari M (2018) Removal of toxic methyl green (MG) in aqueous solutions by apricot stone activated carbon – Equilibrium and isotherms modeling. *Desalination and Water Treatment* 125: 93–101.

Abbas M, Harrache Z and Trari M (2019) Removal of gentian violet in aqueous solution by activated carbon equilibrium, kinetics, and thermodynamic study. *Adsorption Science & Technology* 37(7–8): 566–589.

Abbas M, Harrache Z and Trari M (2020) Mass-transfer processes in the adsorption of crystal violet by activated carbon derived from pomegranate peels: Kinetics and thermodynamic studies. *Journal of Engineered Fibers and Fabrics* 15: 1–11.

Abbas M and Trari M (2020a). Contribution of adsorption and photo catalysis for the elimination of Black Eriochrome (NET) in an aqueous medium – Optimization of the parameters and kinetics modeling. *Scientific African* 8: e00387.

Abbas M and Trari M (2020b) Removal of methylene blue (MB) in aqueous solution by economic adsorbent derived from apricot stone activated carbon (ASAC). *Fibers and Polymers* 21: 810–820.

Abbas M and Trari M (2020c) Photocatalytic degradation of asucryl red (GRL) in aqueous medium on heat-treated TiO_2 powder – Eeffect of analytical parameters and kinetic modeling. *Desalination and Water Treatment* 180: 398–404.

Ahmed MJ and Dhedan SK (2012) Equilibrium isotherms and kinetics modeling of methylene blue adsorption on agricultural wastes-based activated carbons. *Fluid Phase Equilibria* 317: 9–14.

Ahn D-H, Chang W-S and Yoon T-I (1999) Dyes tuff waste water treatment using chemical oxidation, physical adsorption and fixed bed biofilm process. *Process Biochemistry* 34(5): 429–439.

Attia AA, Girgis BS, Fathy NA, et al. (2008) Removal of methylene blue by carbons derived from peach stones by H_3PO_4 activation: Batch and column studies. *Dyes and Pigments* 76(1): 282–289.

Baccar R, Sarra M, Bouzid J, et al. (2012) Removal of pharmaceutical compounds by activated carbon prepared from agricultural by-product. *Chemical Engineering Journal* 211–212: 310–317.

Baquero MC, Giraldo L, Moreno JC, et al. (2003) Activated carbons by pyrolysis of coffee bean husks in presence of phosphoric acid. *Journal of Analytical and Applied Pyrolysis* 70(2): 779–784.

Berrios M, Martin M and Martin A (2012) Treatment of pollutants in wastewater: Adsorption of methylene blue onto olive-based activated carbon. *Journal of Industrial and Engineering Chemistry* 18(2): 780–784.

Colak F, Atar N and Olgun A (2009) Biosorption of acidic dyes from aqueous solution by *Paeniba cillusmacerans*: Kinetics, thermodynamic and equilibrium studies. *Chemical Engineering Journal* 150(1): 122–130.

Dincer AR, Guner Y and Karakaya N (2006) Coal-based botton ash (CBBA) waste material as adsorbent for removal of iile dyestuffs from aqueous solution. *Colloid and Interface Science* 293: 303–311.

Djilani C, Zaghdoudi R, Modarressi A, et al. (2012) Elimination of organic micropollutants by adsorption on activated carbon prepared from agricultural waste. *Chemical Engineering Journal* 189–190: 203–212.

Freundlich H (1906) Concerning adsorption in solutions. *Zeitschrift fur physikalische chemie-stochiometrie und verwandtschaftslehre* 57: 385–470.

Ghaedi M, Hossainian H, Montazerozohori M, et al. (2011) A novel acorn based adsorbent for the removal of brilliant green. *Desalination* 281: 226–233.

Ghaedj M, Karimi F, Barrazzch B, et al. (2013) Removal of reactive orange 12 from aqueous solutions by adsorption on tin sulfide nanoparticle loaded on activated carbon. *Journal of Industrial and Engineering Chemistry* 19(3): 756.

Harrache Z, Abbas M, Aksil T, et al. (2019) Modeling of adsorption isotherms of (5, 5'-disodium indigo sulfonate) from aqueous solution onto activated carbon: Equilibrium, thermodynamic studies, and error analysis. *Desalination and Water Treatment* 147: 273–283. Vol

Ho YS and McKay G (1998) Kinetic models for the sorption of dye from aqueous solution by wood. *Process Safety and Environmental Protection* 76(2): 183–191.

Juang RS and Chen ML (1997) Application of the Elovich equation to the kinetics of metal sorption with solvent-impregnated resins. *Industrial & Engineering Chemistry Research* 36(3): 813–820.

Karaer H and Uzun I (2013) Adsorption of basic dyestuffs from aqueous solution by modified chitosan. *Desalination and Water Treatment* 51(10–12): 2294–2305.

Kismir Y and Aroguz AZ (2011) Adsorption characteristics of the hazardous dye brilliant green on saklıkent mud. *Chemical Engineering Journal* 172(1): 199–206.

Kyzas GZ, Lazaridis NK and Mitropoulos ACh (2012) Removal of dyes from aqueous solution with untreated coffee residues as potential low-cost adsorbents: Equilibrium, reuse and thermodynamic approach. *Chemical Engineering Journal* 189–190: 148–159.

Lagergren S (1998) About the theory of so-called adsorption of soluble substance. *Kungliga Svenska Vetenskapsakademiens Handlingar* 24: 1–39.

Laine J, Calafat A and Labady M (1989) Preparation and characterization of activated carbons from coconut shell impregnated. *Carbon* 27(2): 191–195.

Langmuir I (1918) The adsorption of gases on plane surfaces of glass, mica and platinum. *Journal of the American Chemical Society* 40(9): 1361–1403.

Laskar N and Kumar U (2019) Removal of brilliant green dye from water by modified *BambusaTulda*: Adsorption isotherm, kinetics and thermodynamics study. *International Journal of Environmental Science and Technology* 16(3): 1649–1662.

Liou T-H (2010) Development of mesoporous structure and high adsorption capacity of biomass-based activated carbon by phosphoric acid and zinc chloride activation. *Chemical Engineering Journal* 158(2): 129–142.

Mittal A, Kaur D and Mittal J (2008) Applicability of waste materials – Bottom ash and deoiled soya – As adsorbents for the removal and recovery of a hazardous dye, brilliant green. *Journal of Colloid and Interface Science* 326(1): 8–17.

Nandi BK, Goswami A and Purkait MK (2009) Adsorption characteristics of brilliant green dye on kaolin. *Journal of Hazardous Materials* 161(1): 387–395.

Nassar MM, El-Geundi MS and Al-Wahbi AA (2012) Equilibrium modeling and thermodynamic parameters for adsorption of cationic dyes onto Yemen natural clay. *Desalination and Water Treatment* 44(1–3): 340–349.

Ragab A, Ahmed I, Bader D, et al. (2019) The removal of brilliant green dye from aqueous solution using nano hydroxyapatite/chitosan composite as a sorbent. *Molecules* 24(5): 847–863.

Saif Ur Rehman M, Munir M, Ashfaq M, et al. (2013) Adsorption of brilliant green dye from aqueous solution onto red clay. *Chemical Engineering Journal* 228: 54–62.

Shirsath SR, Patil AP, Patil R, et al. (2013) Removal of brilliant green from wastewater using conventional and ultrasonically prepared poly(acrylic acid) hydrogel loaded with kaolin clay a comparative study. *Ultrasonics Sonochemistry* 20(3): 914–923.

Suárez-García F, Martínez-Alonso A, Tascón JMD, et al. (2001) Porous iure of activated carbons prepared by phosphoric acid activation of apple pulp. *Carbon* 39(7): 1111–1116.

Sun Y, Yue Q, Gao B, et al. (2012) Comparative study on characterization and adsorption properties of activated carbons with H_3PO_4 and $H_4P_2O_7$ activation employing *Cyperusal ternifolius* as precursor. *Chemical Engineering Journal* 181–182: 790–797.

Tavlieva MP, Genieva SD, Georgieva VG, et al. (2013) Kinetic study of brilliant green adsorption from aqueous solution onto white rice husk ash. *Journal of Colloid and Interface Science* 409: 112–122.

Temkin M and Pyzhev V (1940) Kinetics of ammonia synthesis on promoted iron catalysts. *Acta Physicochim URSS* 12: 327–356.

Valix M, Cheung WH and McKay G (2004) Preparation of activated carbon using low temperature carbonization and physical activation of high ash raw bagasse for acid dye adsorption. *Chemosphere* 56(5): 493–501.

Weber MJ and Morris J (1963) Kinetic of adsorption on carbon from solution. *ASCE Journal of Sanitary Engineering Division* 89: 31–51.

Yagmur E, Ozmak M and Aktas Z (2008) A novel method for production of activated carbon from waste tea by chemical activation with microwave, energy. *Fuel* 87(15–16): 3278–3285.